Effect of Spray Dryer Absorber (SDA) Ash on the Performance of Warm Mix Asphalt (WMA)

Clayton Cloutier[1], Thomas Jansen[2], Robert Meidl[2], Ahmed Faheem[3], Ervin Dukatz[4], Konstantin Sobolev[1]

[1]University of Wisconsin-Milwaukee, Engineering and Applied Sciences, 3200 N. Cramer St., Milwaukee, WI 53211; [2]We Energies, 333 W. Everett St., Milwaukee, WI, 53203; [3]Temple University, 1947 N. 12th St., Philadelphia, PA 19122; [4]Mathy Construction Co., 920 10th Ave. N., Onalaska, WI 54650

CONFERENCE: 2017 World of Coal Ash – (www.worldofcoalash.org)

KEYWORDS: ASHphalt, Warm Mix Asphalt, SDA Ash, Coal Combustion Products

ABSTRACT

The field use of Coal Combustion Products (CCPs) in asphalt pavements (ASHphalt) has been limited. Few researchers have reported on the benefits of CCPs in asphalt and even fewer have reported on the benefits of Spray Dryer Absorber (SDA) materials in asphalt. The SDA materials are byproducts of flue gas desulfurization (FGD) air emission control processes that generally do not meet the ASTM C618 specifications for coal fly ash. This research investigates the effect of SDA material that was collected with subbituminous coal fly ash on asphalt properties with respect to laboratory measured performance indicators at the mixture level using the PG58-28 and PG52-34 unmodified Warm Mix Asphalt (WMA) binders. In this study, the SDA ash was introduced to an asphalt mixture at 10% binder replacement (by volume) and then compared to control mixtures. A 12.5 mm maximum aggregates blend was used to evaluate the characteristics of mixture. With respect to performance, all mixtures were tested for workability, aging resistance, indirect-tension capacity, moisture damage resistance, fatigue resistance, and low-temperature thermal cracking resistance.

1. INTRODUCTION

Today, building a durable and cost efficient infrastructure while minimizing future repair needs and expenses is a challenging task, and innovative technological breakthroughs are needed. According to the American Coal Ash Association, in 2015, 117 million tons of Coal Combustion Products (CCPs) were produced in the USA, but only 52% were beneficially utilized. The remaining 48% went to landfills or alternative disposal settings. Moreover, only 0.13% was utilized as mineral additive in asphaltic concrete pavement. Out of approximately 1.31 million tons of SDA produced in the USA only 19.3% are currently being used, mainly in mining applications and the oil/gas field services industries. This leaves 80.7% of the material to be disposed in landfills. New markets and innovative uses of CCPs, especially SDA materials, are needed to increase the beneficial utilization of byproducts that otherwise will be disposed in landfills.[1]

The Spray Dryer Absorber (SDA) materials are byproducts of some flue gas desulfurization (FGD) air quality control systems often referred to as SDA scrubbers. SDA scrubber systems typically use aqueous calcium or sodium based reagents as sorbents to reduce the sulfur dioxide (SO_2) emissions from the flue gasses at coal-fired power plants. Depending on where the sorbents are injected in the process, the SDA system byproducts may be removed from the flue gas and captured with the coal fly ash or downstream of the main fly ash removal device.[2]

Construction material researchers have investigated the use of byproducts such as fly ash to improve the properties of asphalt.[3] Fly ash has been used extensively in portland cement concrete technology; however, there are limited applications in which fly ash has been tested in asphalt pavements.[4,5,6,7,8,9,10]

Sobolev et al. reported that the introduction of fly ash into Hot Mix Asphalt (HMA) mixtures (ASHphalt) improves the performance at levels compared with those achieved through polymer modification.[8] This is attributed to the unique spherical, beneficial size distribution and chemical properties of fly ash. The use of fly ash in bitumen based materials is attractive as it improves the performance and reduces the costs and environmental impacts. Advantages of fly ash in asphalt include improved mixing, placing and compaction, stability, resistance to water damage, rutting resistance, flexibility, and resistance to freeze-thaw damage.[11]

Bautista et al. conducted a series of performance tests on HMA mastics. A large group of CCPs at different concentrations were mixed with different unmodified asphalt binders and on different levels of polymer modifications. They found that most of the influence of the CCPs was not binder dependent. This could be due to the increased sulfur content of some of the CCPs that were used in the study.[12]

Despite these reported benefits, the application of fly ash in asphalt technology has not been widely utilized beyond use in stone matrix asphalt pavement. The use of fly ash has received most of the research focus, while SDA material and specifically SDA ash have not been thoroughly explored for use in asphalt mixtures.

1.1 FIELD IMPLEMENTATION

In the summer of 2016, a 1.61 km road near Wausau, Wisconsin was paved using various control asphalt mixtures and ASHphalt mixtures. In this project, there were two 0.50 km pavement sections with 3.96 m lane widths. One section used a 4-MT WMA ASHphalt mixture (12.5 mm max aggregate size) with PG58-28 binder at 10% SDA ash replacement by binder volume in a 50.8 mm surface layer. The other section used a 4-MT WMA ASHphalt mixture (12.5 mm max aggregate size) with PG52-34 binder at 10% SDA ash replacement by binder volume in a 50.8 mm surface layer. Both test sections were placed on a 101.6 mm base layer using 2-MT HMA (Hot Mix Asphalt) ASHphalt mixture (25.0 mm max aggregate size) with PG58-28 binder at 10% SDA ash replacement by binder volume. Both test sections were placed and compacted with no apparent qualitative difference in flow from truck beds, flow through the paving equipment, compaction effort, labor, and cleaning of equipment.

Over 11,000 quad-axle truckloads used the haul road over a five-month period that was during record setting hot summer temperatures in 2016. Visual inspections indicated no observed rutting of the pavement test sections. Visual inspections were performed during the winter of 2017, and there was no observed indication of low-temperature cracking. The lowest recorded temperature for the season was -26^{o}C.

1.2 LABORATORY RESEARCH STUDY

This research study investigates the control and ASHphalt mixtures used in the Wausau Field Implementation Study. The purpose of this laboratory research is to evaluate the effect of SDA ash from the combustion of subbituminous coal on asphalt performance with respect to laboratory measured performance indicators at the mixture level using PG58-28 and PG52-34 unmodified Warm Mix Asphalt (WMA) binders. In this study the SDA ash was introduced to an asphalt mixture as an enhancer that replaces 10% of the binder by volume and then these mixtures were compared to control mixtures. A 12.5 mm maximum aggregate blend was used to evaluate mixture characteristics.

2. MATERIALS AND TESTING METHODS

This section explains the experimental testing matrix for both the control asphalt mixtures and the ASHphalt mixtures in terms of aggregate coating, workability, aging resistance, moisture damage resistance, fatigue-cracking resistance, and low-temperature thermal-cracking resistance. Table 1 presents the experimental testing matrix for the entire project along with the materials used for this project. For all these tests, at least two samples were tested and averages were determined. For the aggregate coating, workability, and aging comparison, six replicates were produced and compared. For the moisture damage resistance, fatigue cracking resistance, and thermal cracking resistance, two replicates were produced and tested. The experimental testing methods are described in detail in the next sections.

TABLE 1: Experimental Research Testing Matrix

Test	Measured Indicator		Aging	Mixture Types	SDA Ash Dosage	Replicates per Test	Total
Aggregate Coating	Asphalt Binder Film Thickness		Short-Term	• 4-MT (W) • 4-MT (WA) • 4-MT (WAL)	10% of Binder Replacement by **VOLUME**	6	18
Workability	%Air at 8 Gyrations		Short-Term			6	18
Aging Comparison			Long-Term			6	18
Moisture Damage	Tensile Strength Ratio	Dry	Long-Term			2	6
		Saturated				2	6
		Conditioned				2	6
Fatigue	Number of Cycles Drop in E* using IDT	Intermediate Temperature	Long-Term			2	6
Thermal Cracking	Fracture Energy	Low Temperature	Long-Term			2	6
						Total	**84**

* 4-MT = 12.5 mm Max Aggregate Size
* A = SDA Ash Replacement
* L = Low Temperature Binder Grade (PG52-34)
* W = Warm Mix Asphalt

2.1 MATERIALS

For mixture testing, the SDA ash was introduced to an asphalt mix at 10% replacement of the binder by volume. Mixtures prepared for this study used a job mix formula (JMF) approved by the Wisconsin DOT. There were 3 different mixtures total as seen in Table 1. The 4-MT mixtures had a NMAS of 12.5 mm. All the mixtures used a PG58-28 binder (WMA) except for one mixture which used a PG52-34 low temperature binder grade. The 4-MT WMA control mix design had a 5.6% optimum asphalt content and the 4-MT WMA ASHphalt mixture design had a 10% SDA binder replacement so the asphalt binder content was reduced to only 5.0%. The SDA ash was assumed as part of the binder volume rather than as an aggregate component. A control mix was used to compare the impact of the added SDA ash on the performance indicators of mixtures. The control mixes were fabricated according to the JMF at the optimum asphalt content.

The X-Ray Diffraction (XRD) was used to evaluate the SDA ash, and these results can be seen in Figure 1. It was discovered from the XRD analysis that the samples had high backgrounds and low intensity peaks which suggests an abundance of amorphous glass phases. It was also discovered that quartz was the dominant phase for the dry SDA.

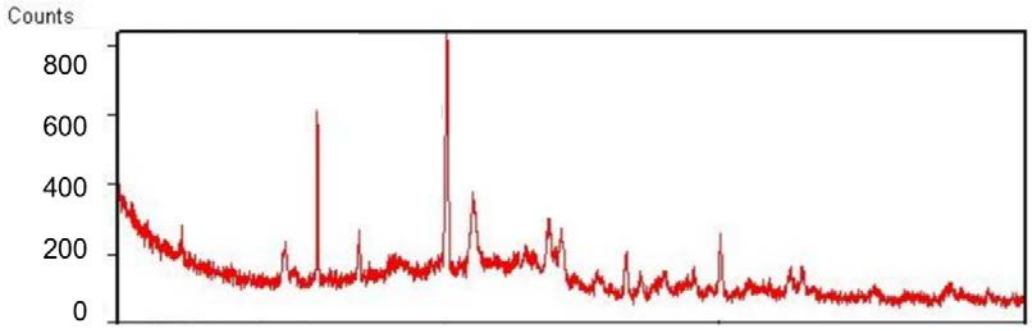

FIGURE 1: The X-ray Diffractogram of SDA

The chemical properties of the SDA ash can be seen in Table 2. This table shows the weighted percentages (total of all percentages equals 100%) for all components in the SDA ash demonstrating that the major component was SiO_2 (31.63%) which correlates with the XRD analysis results. Other major components in this CCP were CaO (25.45%), Al_2O_3 (15.58%), and SO_3 (10.52%).

TABLE 2: Chemical Properties of SDA Ash Material

Component	Weight %	Component	Weight %
SiO_2	31.63	P_2O_5	0.96
Al_2O_3	15.58	Mn_2O_3	0.02
Fe_2O_3	4.56	SrO	0.29
CaO	25.45	BaO	0.51
MgO	4.33	Cr_2O_3	0.01
SO_3	10.52	ZnO	0.02
Na_2O	1.34	Chlorine	0.08
K_2O	0.50	ZrO_2	0.08
TiO_2	1.09	L.O.I (@950 C)	3.02

2.2 AGGREGATE COATING

Aggregate coating was evaluated based on physical observations. Since the total binder content for the ASHphalt mixtures was reduced by 10% by volume, it was important to evaluate the aggregate coating to ensure proper performance. The mixing and compaction temperatures for mix fabrication were determined according to AASHTO T312-12. The control and ASHphalt mixtures were all mixed at 115^{o}C which guaranteed that samples were fabricated at the same viscosity regardless of the mix components.

2.3 WORKABILITY (COMPACTION)

The workability was evaluated in accordance to AASHTO T312-12. The compaction densification curves were compared for the control mixtures and the ASHphalt mixtures.

All mixtures were compacted using a Superpave® Gyratory Compactor to 100 gyrations to evaluate the compaction performance over a wide range of gyrations. The WMA mixtures were compacted at 115°C. Each mixture was compacted using a 150 mm diameter mold with a vertical pressure of 600 kPa and a gyration angle of 1.25°. All compaction comparisons for workability were evaluated using the short-term aged materials to demonstrate the physical condition in which the material is mixed, placed, and compacted. In this way, lower compaction effort demonstrated a better workability properties.

2.4 AGING RESISTANCE

The aging resistance was evaluated by comparing the aging index of all the mixtures. The aging index was calculated as the difference in air content at 8 gyrations for long-term aged materials versus the air content at 8 gyrations for short-term aged materials:

$$Aging\ Index = A\%_{LT} - A\%_{ST} \quad \text{Eq. 1}$$

where:

$A\%_{LT}$ = Number of gyrations to reach 92% G_{mm} for long-term aged materials;
$A\%_{ST}$ = Number of gyrations to reach 92% G_{mm} for short-term aged materials.

The short-term aged materials were placed in a forced-draft oven for 2 h ± 5 min at a temperature of 115°C ± 3°C (compaction temperature). This procedure was followed in accordance to AASHTO R30-02. The long-term aged materials were placed in a force-draft oven for 24 ± 0.5h at a temperature of 115°C ± 3°C (compaction temperature for WMA).

The short-term aging procedure used in this research mimics the aging due to mixing, placing, and compacting whereas the long-term aging procedure used in this research represents 8 to 10 years of aging in the field. Comparing the material in these different aging conditions was critical because resisting the effects of age-hardening could potentially increase the life expectancy of the material since it would become stiffer at a slower rate. The long-term aged procedure was in accordance to AASHTO R30-02 and methods adapted by Elwardany, Rad, Castorena, & Kim.[13]

2.5 MOISTURE DAMAGE

Moisture damage resistance was evaluated in accordance to AASHTO T283-07. Samples were core drilled to a 101.6 ± 2.0 mm diameter and then cut to a thickness of 50.8 ± 2.0 mm. A saturated sample was compared to a conditioned sample to evaluate the Tensile Strength Ratio (TSR) using the Indirect Tension Test (IDT). Both the saturated and conditioned samples were saturated to a degree of saturation of 70-80%.

The saturated samples were saturated to reach the appropriate range of 70-80%, then placed in a water bath at 25 ± 0.5°C for 2 h ± 10 min with a minimum of 25 mm of water above the surface of the specimen and then tested for IDT. The conditioned samples were saturated to the appropriate range of 70-80%, then placed in a water bath at 60°C

± 1°C for 24 ± 1 hr. After 24 ± 1 h, the specimens were removed from the water bath and then placed into a different water container at 25 ± 0.5°C for 2 h ± 10 min with a minimum of 25 mm of water above the surface of the specimen and then tested for IDT.

The TSR was then calculated as the ratio of the ultimate strength of the conditioned samples versus the ultimate strength of the saturated samples:

$$TSR = \frac{S_c}{S_s} \quad \text{Eq. 2}$$

where:

S_c = average tensile strength of conditioned specimen (MPa);
S_s = average tensile strength of saturated specimen (MPa).

The equation for tensile stress and tensile strain were also developed[14,15,16] as reported below:

$$\sigma_x = \frac{2P}{\pi dt} \quad \text{Eq. 3}$$

where:

σ_x = horizontal tensile stress at center of specimen, (MPa);
P = applied load, (N);
d = diameter of specimen, (mm);
t = thickness of specimen, (mm).

$$\varepsilon_f = 0.52 x_t \quad \text{Eq. 4}$$

where:

ε_f = tensile strain at failure (mm/mm);
xt = horizontal deformation across the specimen (in.).

2.6 FATIGUE RESISTANCE

Fatigue testing was performed as a modified test from AASHTO T322-03, AASHTO T342-11, and methods adapted by Shu et al.[17] Typical results of fatigue tests are reported in Figure 2. The repeated cyclic indirect tension (IDT) loading yielded a deformation curve that shows early rapid deformation (initial flow) followed by steady state rate of deformation (secondary flow), then when the samples undergo the failure, the rate of deformation increases again (tertiary flow). The performance parameters for this test are the secondary flow steady rate of deformation.

Fatigue cracking resistance was evaluated to understand the number of cycles each specimen could withstand prior to failure. The fatigue test that was used to evaluate the slope of the secondary fatigue section as well as the failure point (N_f) which is where the tertiary fatigue section started. It was determined that at this point, the Complex Modulus (E*) started to decrease since the slope of the deformation (strain) line increased. Asphalt pavements that demonstrated smaller deformation rates and higher amounts of cycles until failure were considered desirable.

The Complex Modulus, E*, can be determined by evaluating the stress and strain rate at different locations. By calculating the ratio of the stress amplitude and the strain-rate from the cyclic test, the dynamic modulus is represented as:

$$E^* = \frac{\sigma_o}{\varepsilon_o} \quad \text{Eq. 5}$$

where:

σ_o = stress amplitude (MPa);
ε_o = strain-rate (mm/cycle).

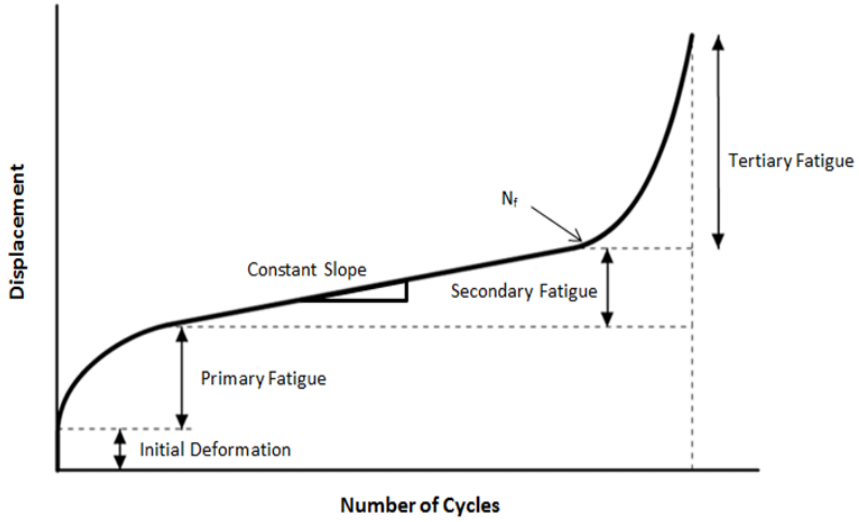

FIGURE 2: Typical Deformation Plot for Repeated Fatigue Loading

For this study, fatigue was evaluated by using a sine wave indirect tension loading condition, a test temperature of 20 ± 1ºC, a 2% pre-loading condition, a 25% ultimate loading condition, and a frequency of 10 Hz. Dry samples of 101.6 ± 2.0 mm diameter by 50.8 ± 2.0 mm thick were tested in IDT to determine the ultimate load used for the testing. For evaluation, the ultimate load of the control sample was used for the 2% and 25% loading conditions. To evaluate the fatigue cracking resistance, a universal loading frame was used with an environmental chamber with temperature control capability. The applied load and vertical displacement was recorded to calculate the needed performance indicators.

2.7 THERMAL-CRACKING RESISTANCE

The Semi-Circular Bending (SCB) test was used to determine the low-temperature properties (at -18ºC) such as Fracture Energy (G_f) and Stiffness (S). Asphalt mixtures become brittle at low temperatures, and when the thermal stresses become too large, the pavement cracks as a result. Therefore, asphalt materials that are too brittle at low temperature are undesirable, whereas materials that remain more elastic at low temperatures perform better since these are able to recover from the emerging

stresses. The G_f is obtained by dividing the work of fracture (area under the load vs. vertical displacement curve) by the ligament area:

$$G_f = \frac{W_f}{A_{lig}} \quad \text{Eq. 6}$$

$$W_f = \int Pdu = W + W_{tail} \quad \text{Eq. 7}$$

$$A_{lig} = (r - a) * t \quad \text{Eq. 8}$$

Where:

$W_f = \int Pdu = W + W_{tail}$, work of fracture (J);
P = applied load (N);
u = load line displacement (m);
A_{lig} = ligament area (m^2);
r= specimen radius (m);
a = notch length (m);
t = specimen thickness (m);

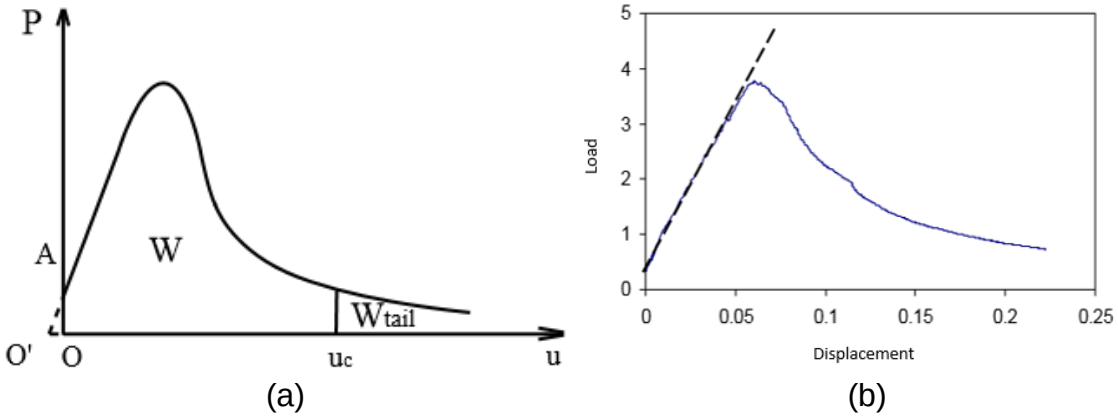

(a) (b)

FIGURE 3: (a) Low-Temperature Load vs. Load-Line Displacement Representation (b) Stiffness (S) Determination of Low-Temperature Testing

The Stiffness (S) is represented as the slope of the linear portion of the vertical displacement curve which can be seen in Figure 3b.

For this testing, higher values of G_f are desirable as this demonstrates larger amounts of energy necessary to crack the specimen. On the other hand, lower stiffness values are desirable as this demonstrates a more ductile material that can recover from the stresses that are developed due to traffic loads. The SCB test was performed at -18°C by applying a vertical load on the specimen at a rate of 0.03 mm/min, and the test was finished once the load decreased to 0.5 kN.

3. RESEARCH RESULTS

3.1 AGGREGATE COATING

Aggregate coating was evaluated to ensure that the aggregates were properly coated, especially since the ASHphalt samples were compacted with 10% less binder (by volume). Figure 4 shows particles coated with asphalt for both ASHphalt and control mixtures. It was observed that the mixing resulted in uniform coating of particles without the need for altering mixing time or technique. This result is due to the volume extension of the binder by means of the CCP particles.

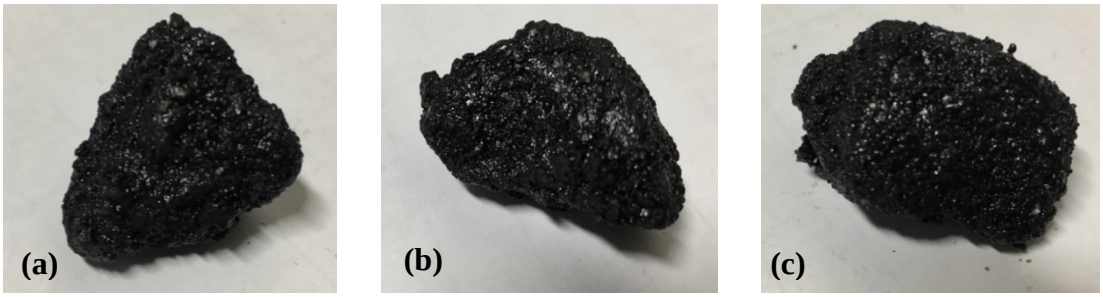

FIGURE 4: Aggregate Coating (a) 4-MT WMA Control (b) 4-MT WMA ASHphalt (c) 4-MT WMA ASHphalt (PG52-34)

3.2 WORKABILITY (BY COMPACTION)

Figure 5 demonstrates the workability results for 4-MT (12.5 mm max aggregate size) WMA mixtures with a PG58-28 binder and a PG52-34 binder. The 4-MT ASHphalt mixture with PG52-34 binder required the least amount of compaction effort when compared to all other mixtures. The 4-MT ASHphalt mixture with PG58-28 binder demonstrated that the compaction efforts towards the beginning (93% G_{mm}) were lower than the control mixture but then over time the slope of the densification curve is reduced below that of the control mixture which means that it takes more compaction energy to deform the material. This means that over time, the material behaves in a stiffer manner at elevated temperatures (this can be correlated to improved rutting resistance) without compromising workability.

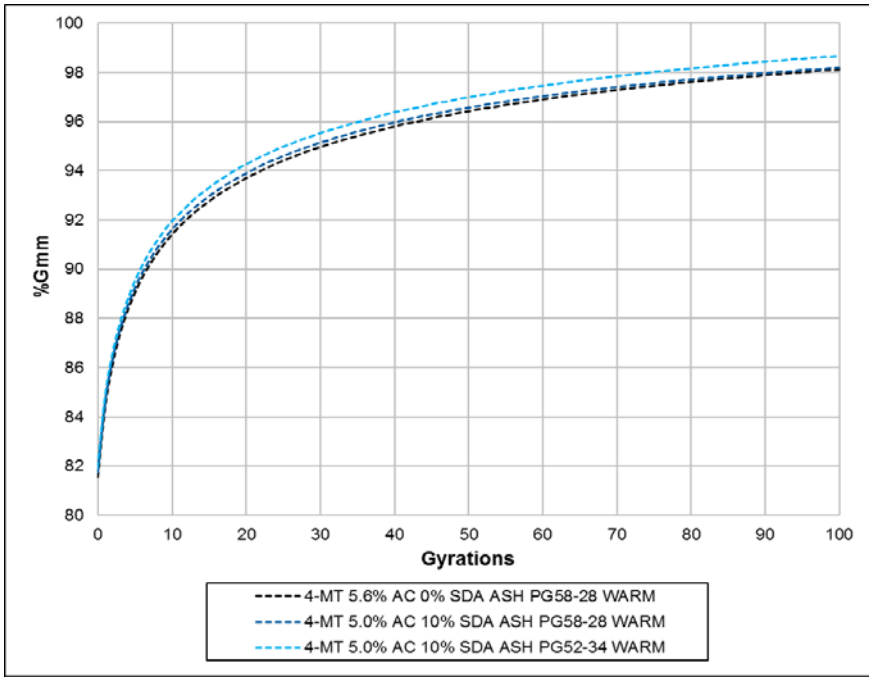

FIGURE 5: The Densification Curve for 4-MT WMA

The compaction volumetrics were evaluated to understand the differences between the control and ASHphalt mixtures. Table 3 shows the mixture volumetrics for the 4-MT WMA mixtures. From this table, Other volumetrics that demonstrate the differences are the added binder content (P_b), voids in the mineral aggregate (VMA), air voids (V_a), voids filled with asphalt (VFA), and the dust-to-binder ratio. Since 10% (by volume) of asphalt content was being replaced with SDA ash, the, voids in the mineral aggregate, and the voids filled with asphalt were all reduced as a result. However, considering that more SDA ash “dust powder” (material that passes the No. 200 sieve) was added to the ASHphalt mixtures, the dust-to-binder ratio increased as a result when compared to the control mixture.

When evaluating the Superpave® volumetric mixture design requirements it was noted that the VMA needs to be above 14% for 4-MT mixtures. Other design parameters require that the VFA needs to be between 65 and 75% (3 to < 30, 30 ≤ ESALs in millions) for all mixtures, and the dust-to-binder ratio needs to be between 0.6 and 1.2 for all mixtures. Evaluating the mixture volumetrics it can be observed that for all mixtures, these parameters are satisfied.

TABLE 3: 4-MT WMA Mixture Volumetrics

Mixture	4-MT 5.6% AC 0% SDA ASH PG58-28 (Warm Mix)	4-MT 5.0% AC 10% SDA ASH PG58-28 (Warm Mix)	4-MT 5.0% AC 10% SDA ASH PG52-34 (Warm Mix)
Gmm	2.458	2.469	2.468
Gmb	2.359	2.370	2.369
Gsb	2.667	2.667	2.667
Gse	2.686	2.686	2.686
Gb	1.028	1.028	1.028
Design Pb (%)	5.6	5.0	5.0
Pba (%)	0.3	0.3	0.3
Ps (%)	94.4	95.0	95.0
Pbe (%)	5.3	4.7	4.7
VMA (%) > 14	16.5	15.6	15.6
Va (%) = 4.0%	4.0	4.0	4.0
VFA (%) (65-75)	75.7	74.3	74.4
Dust-to-Binder Ratio (0.6-1.2)	0.8	1.0	1.0

3.3 AGING RESISTANCE

Figures 6 displays the percentage of air for both the short-term and long-term compacted specimens at 8 gyrations (N_{ini}). Age-hardening increases the stiffness of the material which means the compaction effort typically increases. It is important to understand that mixtures with similar percentages of air at 8 gyrations resist the effects of aging. Materials with poor aging resistance reveal higher deviations in percentages of air at different aging conditions. Since there is more air in the long-term aged mixtures at 8 gyrations, these materials demonstrate age-hardening due to the increase in the compaction effort. Materials with positive values for the aging index demonstrate age-hardening and materials with negative values for the aging index demonstrate age-softening.

Figure 6 shows the air contents for the 4-MT WMA mixtures at both the short-term aged and long-term aged condition. Figure 7 shows the aging index for these mixtures. From Figure 7 it can be seen that all of the mixtures developed age-hardening since the values of the aging index are all positive. However, since the ageing index is less that one (1.0) for all mixes, this means that no additional compaction effort is needed due to aging.

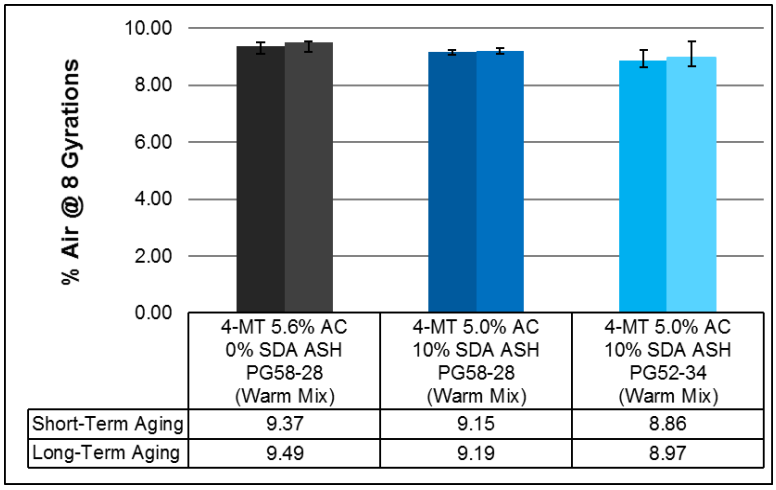

FIGURE 6: The Air Content at 8 Gyrations for 4-MT WMA

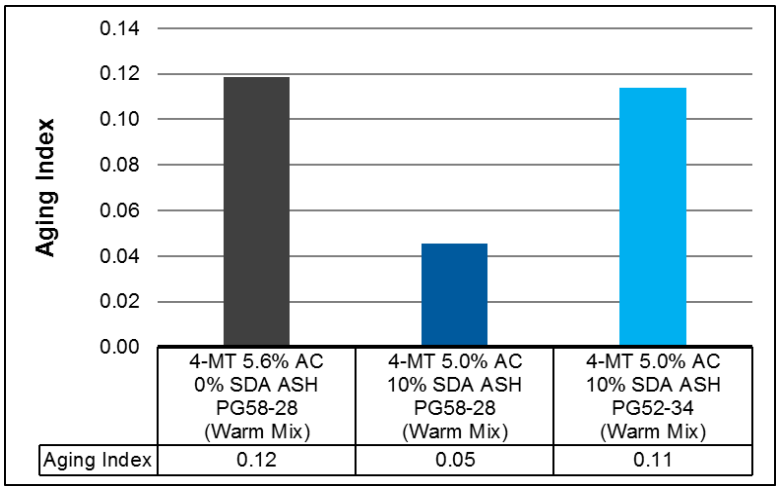

FIGURE 7: The Aging Index for 4-MT WMA

It is important to note that this aging evaluation approach was damage independent and was used only as an indication of potential differences in compaction due to aging. With the results being indiscriminate, it is difficult to assess whether the mixes are showing such low sensitivity to aging or that this approach was unable to truly test the aging effect. Since there is no standard or proposed test in the literature, the research relied more on damage dependent tests, namely moisture damage, fatigue resistance, and low-temperature resistance to evaluate the impact of the SDA material on aging. This is because the results of these tests are highly influenced by the extent of embrittlement in the binder due to oxidative aging.

3.4 MOISTURE DAMAGE

The results of the Indirect Tensile Test (IDT) for dry, saturated, and conditioned samples can be seen in Table 4. These results demonstrate that for all testing conditions, the HMA ASHphalt mixtures with PG58-28 binder developed comparable or higher strengths when compared to the appropriate control mixtures, however, flow (displacement) was reduced in all cases. The load and displacement can be correlated as an inverse relationship. As the maximum load increased, the maximum flow of the sample decreased. The 4-MT WMA dry ASHphalt mixture with PG52-34 developed the lowest ultimate strengths of 8.25 kN. The 4-MT WMA dry control mixture with PG58-28 developed the highest horizontal deformation at failure of 4.04 mm.

For saturated samples, it is interesting to see that the maximum load increased in certain situations as compared to the dry samples even though the samples had a degree of saturation between 70 and 80%. The 4-MT WMA ASHphalt mixture with PG58-28 binder experienced higher ultimate strengths when saturated. These results have to be investigated further to understand the “hydration” contribution of CCP filler.

TABLE 4: The IDT Ultimate Load (kN) and Horizontal Deformation at Failure (mm) of all Mixtures

	Ultimate Load (kN)			Horizontal Deformation at Failure (mm)		
Sample	**Dry**	**Saturated**	**Conditioned**	**Dry**	**Saturated**	**Conditioned**
4-MT 5.6% AC 0% SDA ASH PG58-28 (Warm Mix)	10.79	9.74	8.61	4.04	3.59	3.40
4-MT 5.0% AC 10% SDA ASH PG58-28 (Warm Mix)	10.68	11.05	10.25	3.45	3.39	3.33
4-MT 5.0% AC 10% SDA ASH PG52-34 (Warm Mix)	8.25	7.63	6.83	3.21	2.90	2.81

Figure 8 shows the horizontal tensile stress of the ASHphalt and control samples. These results give a visual correlation to the maximum load results represented in Table 4. From these figures, it can be seen that the maximum horizontal stress for the 4-MT WMA ASHphalt samples with PG58-28 binder were higher than the values of control samples in most cases. The saturated 4-MT WMA mixture with PG58-28 binder had the highest maximum horizontal stress of 1.36 MPa.

Figure 9 shows the tensile strain at failure for the ASHphalt and control specimens. These results give a visual representation of the maximum flow (displacement) results represented in Table 4. This figure demonstrates the effects of moisture damage on the ability for asphalt pavements to deform. For conditioned specimens the strain at failure is reduced in all cases. The 4-MT WMA dry control mixture with PG58-28 experienced the highest strain at failure of 0.083 mm/mm.

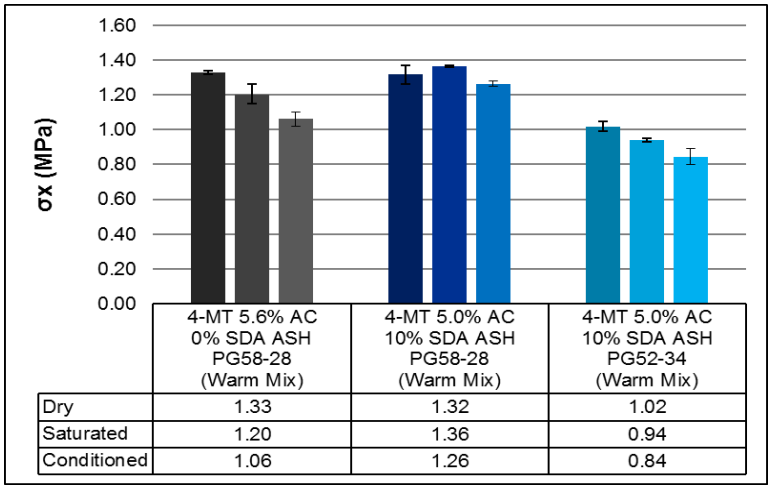

	4-MT 5.6% AC 0% SDA ASH PG58-28 (Warm Mix)	4-MT 5.0% AC 10% SDA ASH PG58-28 (Warm Mix)	4-MT 5.0% AC 10% SDA ASH PG52-34 (Warm Mix)
Dry	1.33	1.32	1.02
Saturated	1.20	1.36	0.94
Conditioned	1.06	1.26	0.84

FIGURE 8 The Horizontal Tensile Stress (MPa) at the Center of the Specimen

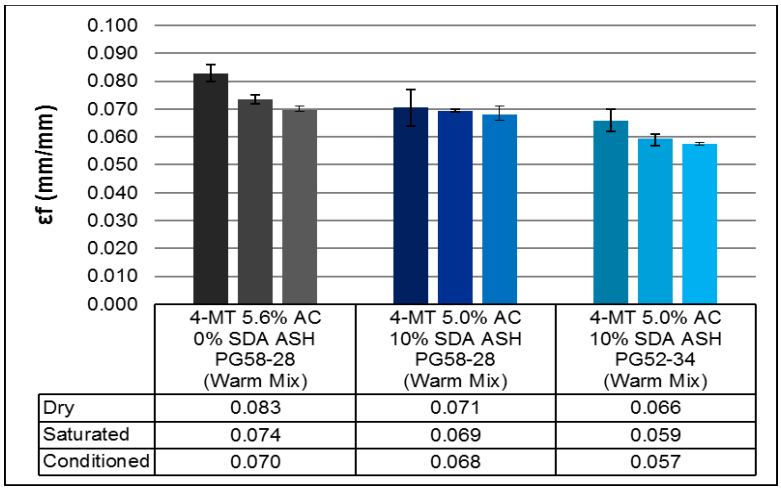

	4-MT 5.6% AC 0% SDA ASH PG58-28 (Warm Mix)	4-MT 5.0% AC 10% SDA ASH PG58-28 (Warm Mix)	4-MT 5.0% AC 10% SDA ASH PG52-34 (Warm Mix)
Dry	0.083	0.071	0.066
Saturated	0.074	0.069	0.059
Conditioned	0.070	0.068	0.057

FIGURE 9: The Horizontal Tensile Strain (mm/mm) at Failure

The Tensile Strength Ratio (TSR) was calculated and compared for conditioned and saturated samples (Figure 10). The TSR values are required to be at or above 80%; the results demonstrate that all mixtures fulfilled this requirement. Higher values of TSR are desired as this indicates a better performance in terms of moisture damage resistance. It can be observed that all ASHphalt mixtures enhanced the moisture damage resistance when compared to the control mixture. The 4-MT WMA control mixture performed the worst with a TSR of 0.884. Yet it is important to note that the most increase in the TSR is just 5%.

In terms of moisture damage resistance, it can be concluded that given the reduction in asphalt content, ASHphalt mixtures resisted the effects of moisture damage as well or slightly better than the control mixtures. The results prove that adding the SDA ash to replace 10% of the asphalt content to asphalt mixtures maintains moisture stripping resistance of the mixture.

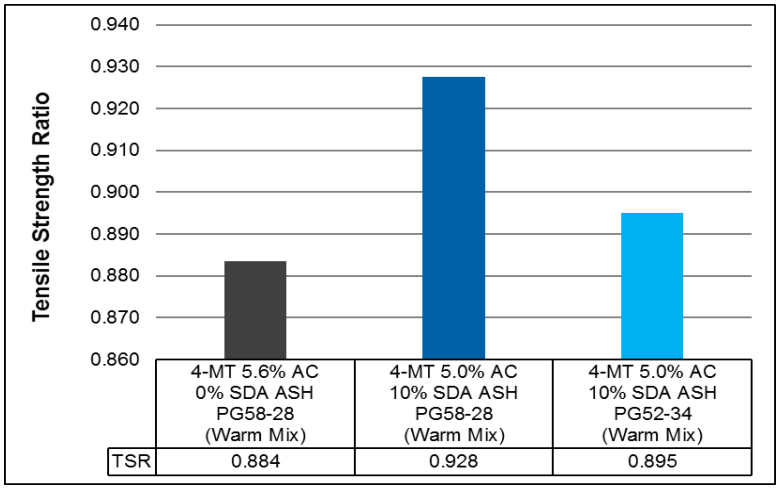

FIGURE 10: Tensile Strength Ratio for all Mixtures

3.5 FATIGUE RESISTANCE

For this study, fatigue was assessed by using a sine wave loading condition, a test temperature of 20 to 25ºC, a 2% pre-loading condition, a 25% ultimate loading condition, and a frequency of 10 Hz. After evaluating the IDT results for the dry samples, it was decided to use an ultimate load of 10.79 kN (2% pre-load = 0.22 kN, 25% ultimate = 2.70 kN) for the 4-MT WMA mixtures. The fatigue test was run until the material failed.

The results of the fatigue testing can be seen in Figures 11 and 12. These results demonstrate the performance of duplicate samples that were tested in fatigue. These figures show the results for the secondary fatigue slopes as well as the number of cycles that the samples could withstand till there was a 50% drop in E* (Complex Modulus). This drop in E* is directly correlated to N_f as this is the defined point of failure as seen from Figure 2.

Figure 11 shows the vertical deformation slope (mm/mm) for the 4-MT WMA mixtures and Figure 12 shows the number of cycles drop in E*. The 4-MT WMA ASHphalt samples with PG58-28 performed better than the control mixtures since the samples were able to withstand 162,500 cycles till there was a drop in E* whereas the control samples were only able to withstand 87,500 cycles. The slopes of the 4-MT WMA samples with PG58-28 in the secondary fatigue sections were also lower (1.00E-05 mm/cycle) than the control samples (1.89E-05 mm/cycle). The 4-MT WMA samples with PG52-34 performed worse than the control samples since these samples were only able to withstand 33,750 cycles till there was a drop in E* and the vertical deformation slopes were 4.8E-05 mm/cycle. This reduction in fatigue resistance can be correlated to the softer binder properties of the PG52-34 asphalt material since the testing temperature is too warm for this binder grade. The intermediate temperature for a

PG58-28 is 19ºC while that of the PG52-34 is 13ºC. Therefore, the testing conditions were biased against the softer binder.

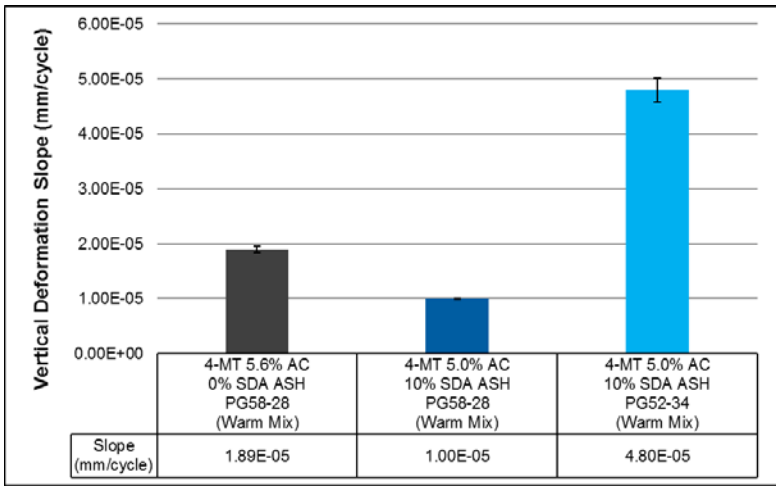

FIGURE 11: The Vertical Deformation Slope (mm/cycle) for 4-MT WMA

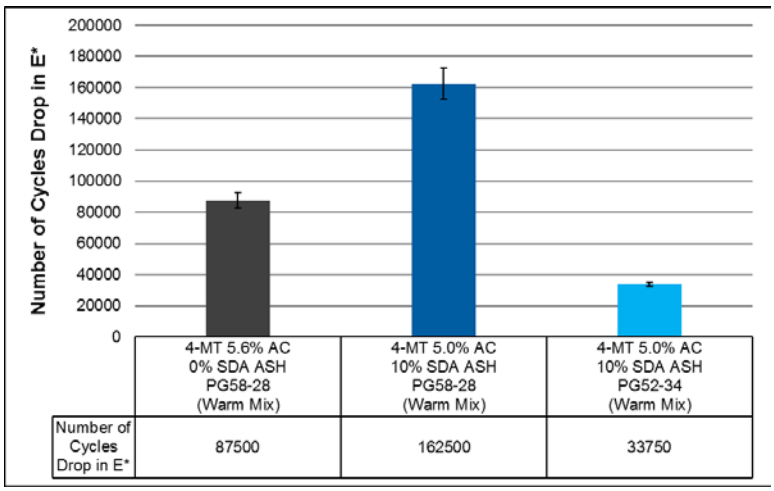

FIGURE 12: The Number of Cycles to 50% Drop in E* for 4-MT WMA

The results of this study prove that WMA ASHphalt mixtures with PG58-28 binder perform better than control mixtures with respect to intermediate-temperature fatigue cracking resistance. Every ASHphalt mixture with PG58-28 binder demonstrated smaller deformation fatigue slopes, and these mixtures were also able to withstand more loading cycles till failure. In more general terms, the results indicate that the SDA is able to improve fatigue resistance of the binder rather than change its grade.

3.6 THERMAL-CRACKING RESISTANCE

The results for the SCB test are shown in Figures 13 and 14. Figure 13 demonstrates the Fracture Energy (G_f) of investigated asphalt materials. As previously mentioned, larger values of G_f are desirable as this demonstrates larger energy required to create a unit surface area of crack. This is obtained by dividing the work of fracture (area under the load vs. load line displacement curve) by the ligament area. From the experimental results, it can be seen that all ASHphalt mixtures performed better than the control mixture in terms of G_f. The 4-MT WMA ASHphalt samples with PG52-34 binder performed the best as this mixture was able to achieve a G_f value of 1.63 kJ/m^2.

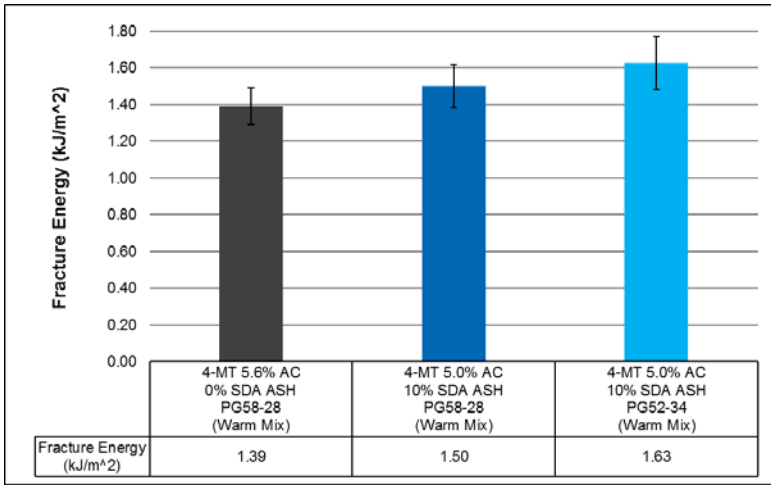

FIGURE 13: The Fracture Energy (Gf) Values for all Mixtures

The comparison between both mixes with PG58-28 asphalt shows a slight (8%) increase in fracture energy. It shows that for the same grade reducing the asphalt content through the help of SDA maintains the mechanical properties of the mix. At the same time the PG52-34 mix does not show that the addition of SDA jeopardized its superior low temperature tolerance.

The Stiffness (S) is represented as the slope of the linear portion of the load-line displacement curve. Lower stiffness values are desirable since this demonstrates a more elastic material that can recover from low-temperature stress accumulations. Figure 14 shows the stiffness results from the SCB testing. From these results, it can be seen that all ASHphalt mixtures performed better than the corresponding control mixtures since the stiffness values were much lower. The 4-MT WMA ASHphalt mixture with PG52-34 binder demonstrated the lowest stiffness of 9.13 kN/mm whereas the 4-MT control mixture obtained the highest stiffness of 11.99 kN/mm. These results reveal that the control samples were much more brittle at the low temperature as compared to the ASHphalt mixtures which behaved more elastically. The mixtures with the PG52-34 binder demonstrated the best results when compared to the other mixtures and this makes sense because this lower binder grade acts as a softer material at lower temperatures. The stiffness results are crucial to this study. Historically, the literature

reports that the addition of fine particles to asphalt results in increased stiffness which has detrimental effect on low temperature performance. The results in Figure 14 proves that the effect of SDA is opposite to these reports.

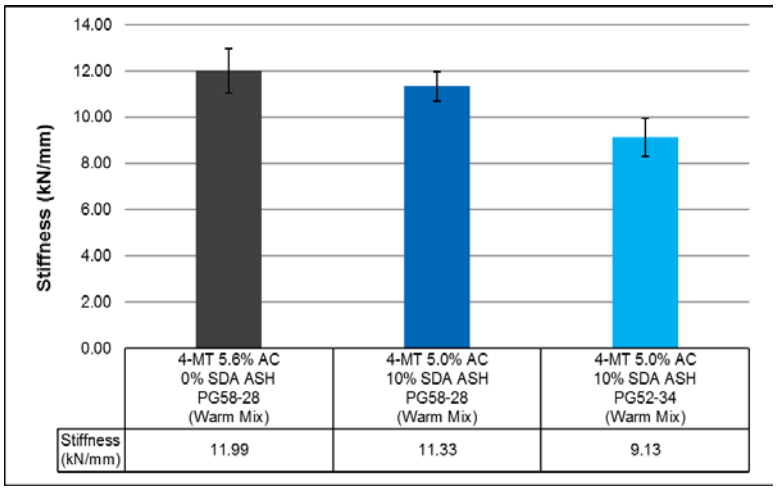

FIGURE 14: Stiffness (S) Values for all Mixtures

In terms of thermal cracking resistance, it can be concluded that ASHphalt mixtures resisted the effects of low-temperature cracking better than the control mixtures in terms of Fracture Energy (Gf) and Stiffness (S). These results prove that adding SDA ash to asphalt mixtures enhances low-temperature thermal cracking resistance.

4. CONCLUSIONS

This research produced very promising results which can be used to increase the acceptance and use of CCPs in ASHphalt pavements. The conclusions and findings can be summarized as follows:

1. Aggregate coating was not hindered for ASHphalt mixtures even though 10% binder (by volume) was replaced with SDA ash. There were no major differences observed for aggregate coating quality or mixing performance. This result is due to the volume extension of the binder by means of the CCPs particles.
2. The workability was used to evaluate the differences in compaction efforts for ASHphalt and control mixtures (WMA compacted at 115^{o}C). The ASHphalt mixtures did not show change in compaction effort at the lowered asphalt content. The 4-MT WMA ASHphalt mixture with PG52-34 binder needed the least amount of compaction effort. The 4-MT WMA ASHphalt mixtures demonstrated an ideal performance in that these materials compacted initially with less effort time (corresponding to service life). This demonstrates that the material is easier to compact out in the field but then requires more compaction effort over time as compared to the control mixtures and then required more compaction effort over to permanently deform the mixture (i.e. less deformations due to vehicle loads) which is associated with improved rutting resistance.

3. Mixture aging testing was not able to discriminate between the mixes since all mixtures achieved aging index less than 1.0. Meaning that no need of additional compaction is required even after ageing for 24hrs.
4. It was demonstrated that the 4-MT WMA ASHphalt samples with PG58-28 binder produced higher ultimate strengths in most cases in Indirect Tensile Testing (IDT) than the control samples. The saturated 4-MT WMA ASHphalt samples with PG58-28 binder developed the highest strengths of 11.05 kN. The dry 4-MT WMA with PG58-28 binder demonstrated the highest ultimate deformation at failure of 4.04 mm which is correlated to higher binder content in the mixture.
5. The research results demonstrated that all ASHphalt mixtures had improved moisture-damage resistance based on the Tensile Strength Ratio (TSR) parameter as compared to the appropriate control mixtures. The 4-MT WMA ASHphalt with PG58-28 binder had the highest TSR of 0.928 and the 4-MT WMA control mixture with PG58-28 binder had the lowest TSR of 0.884.
6. PG58-28 binder performed considerably better than the appropriate control mixtures. The secondary fatigue deformation rate of the 4-MT HMA ASHphalt mix was the lowest deformation rate of 1.00E-05 mm/cycle in the vertical direction. The 4-MT WMA ASHphalt mixtures with PG58-28 binder also performed better than the control mixtures in terms of number of cycles to failure. This mix show increased fatigue life of about 87% more than the control mix. Using SDA show the greatest influence on mixtures performance for fatigue testing.
7. The low-temperature testing show significant results favoring the use of SDA. At 10% less asphalt the fracture energy of the PG58-28 mixture as well as the stiffness show statistically no change when compared to the Control Mix. Furthermore, the softer binder mix show no loss in its ability to mitigate the effect of low temperature when fraction of the asphalt is replaced the SDA.
8. Overall, the use of SDA show a sustainable approach in reducing the asphalt content in mixtures while maintaining or improve the bulk mechanical properties.

5. REFERENCES

[1] American Coal Ash Association. 2015. https://www.acaa-usa.org. Accessed October 18, 2016.

[2] EPRI 2007. A Review of Literature Related to the Use of Spray Dryer Absorber Material: Production, Characterization, Utilization Applications, Barriers, and Recommendations. EPRI, Palo Alto, CA and UND EERC CARRC, Grand Forks, ND: 2007. 1014915.

[3] Sobolev, K., and Naik, T.R. 2005.Performance as a Factor for Sustainability of the Cement Industry. CANMET/ACI International Symposium on Sustainable Development of Cement and Concrete. Toronto, Canada, 295 - 312.

[4] Ali, N., Chan, J.S., Simms, S., Bushman, R., and Bergan, A.T. 1996. Mechanistic evaluation of fly ash asphalt concrete mixtures. Journal of Materials in Civil Engineering, 8 (1): 19-25.

[5] Churchill, E.V., and Amirkhanian, S.N. 1999. Coal ash utilization in asphalt concrete mixtures. Journal of Materials in Civil Engineering, 11 (4): 295-301.

[6] Asi, I., and Assa'ad, A. 2005. Effect of Jordanian oil shale fly ash on asphalt mixes. Journal of Materials in Civil Engineering, 17 (5): 553-559

[7] Faheem, A. F., & Bahia, H. U. (2009). Modelling of Asphalt Mastic in Terms of Filler-Bitumen Interaction. Road Materials and Pavement Design 11 (sup1), 281-303.

[8] Sobolev, K., Ismael, F., Bohler, J., Faheem, A., & Covi, A. (2013). Application of Fly Ash in ASHphalt Concrete from Challenges to Opportunities. Milwaukee, WI.

[9] Bautista, E. G., (2015). Experimental Evaluation of the Effect of Coal Combustion Products on Constructability, Damage and Aging Resistance of Asphalt Mastics. Doctoral Thesis. University of Wisconsin-Milwaukee.

[10] Cloutier, C. J., (2016). The Effective Use of Coal Combustion Products (CCPs) in Asphalt Pavements. Master's Thesis. University of Wisconsin-Milwaukee.

[11] Tapkin, S., (2008). Improved Asphalt Aggregate Mix Properties by Portland Cement Modification. Can. J. Civ. Eng. 35: 27-40.

[12] Bautista, E. G., Faheem, A. F., Saha, R., Sobolev, K. (2015). Characterization of Damage and Aging Resistance of Asphalt Mastics with Coal Combustion By-Products. American Society of Civil Engineers (ASCE) International Airfield & Highway Pavements Conference, June 2015.

[13] Elwardany, M. D., Rad, F. Y., Castorena, C., & Kim, Y. R. (2010). "Evaluation of Asphalt Mixture Laboratory Long-Term Aging Methods for Performance Testing and Prediction". *Cooperative Highway Research Program.* Project No. 9-39, National Research Council, Washington, D.C.

[14] Anagnos, J. N., Kennedy, T. W. (1972). "Practical Method of Conducting the Indirect Tensile Test". *Center for Highway Research.* University of Texas, Research Report 98-10.

[15] Hadley, W. O., Hudson, W. R., & Kennedy, T. W. (1970). "A Method of Estimating Tensile Properties of Materials Tested in Indirect Tension. *Center for Highway Research*. University of Texas, Research Report 98-7.

[16] Hadley, W. O., Hudson, W.R., & Kennedy, T. W. (1972). "An Evaluation of Factors Affecting the Tensile Properties of Asphalt-Treated Materials". *Center for Highway Research.* University of Texas, Research Report 98-2.

[17] Shu, X., Huang, B., & Vukosavljevic, D. (2007). "Laboratory Evaluation of Fatigue Characteristics of Recycled Asphalt Mixtures". *Department of Civil and Environmental Engineering.* University of Tennessee, Knoxville, TN.